

DC AND TERAHERTZ RESPONSE IN Nb SIS MIXERS WITH NbTiN STRIPLINES

B.D. Jackson^{1,2}, N.N. Iosad¹, B. Leone¹, J.R. Gao², T.M. Klapwijk³

W.M. Laauwen², G. de Lange², H. van de Stadt²

¹ *University of Groningen, Department of Applied Physics and Materials Science Centre,
Nijenborgh 4.13, 9747 AG Groningen, The Netherlands*

² *Space Research Organization of the Netherlands, PO Box 800,
9700 AV Groningen, The Netherlands*

³ *Delft University of Technology, Department of Applied Physics (DIMES)
Lorentzweg 1, 2628 CJ Delft, The Netherlands*

Abstract

It is expected that the integration of NbTiN striplines with Nb-based SIS junctions will extend the range of operation of sensitive SIS mixers up to the energy gap of NbTiN (~ 1.2 - 1.25 THz) to meet the requirements of the HIFI instrument for the Far-Infrared Space Telescope (FIRST). We have fabricated prototype SIS waveguide mixers in which Nb/Al-AlO_x/Nb SIS junctions are integrated with NbTiN and Al wiring layers. DC current-voltage measurements of these devices show that the voltage gap is somewhat lower and the sub-gap current is somewhat higher for devices with two NbTiN wiring layers in comparison with those in which the top wiring layer is Al ($V_{\text{gap}} = 2.7$ mV vs. 2.8 mV, and $R_{2,0}/R_N \sim 32$ vs. 35). Additionally, the gap voltage of the NbTiN stripline devices is further suppressed by the application of 890-1040 GHz local oscillator power during heterodyne measurements. These effects are attributed to the trapping of heat in the Nb junction electrodes due primarily to quasi-particle trapping at the Nb/NbTiN interface. FTS measurements result in what is believed to be the first reported observation of direct detection response in a NbTiN stripline device above 1.1 THz. From an analysis of the resonance frequencies of several devices, it appears that the frequency response of the NbTiN striplines is predicted reasonably well by the Mattis-Bardeen theory for the conductivity of a superconductor in the extreme anomalous limit. Furthermore, we present what is believed to be the first reported heterodyne measurements of NbTiN stripline devices in the 0.9-1 THz range. These measurements yield a receiver sensitivity of $T_N = 830$ K at 930 GHz at a bath temperature of 3.3 K, after correction for beamsplitter losses.

1. Introduction

The development of the Heterodyne Instrument for the Far-Infrared Space Telescope (HIFI) requires the development of SIS mixers with noise temperatures below 200 K (DSB) at 1 THz. According to Mattis-Bardeen theory [1], Nb striplines become lossy at frequencies above the Nb gap frequency (~ 680 GHz). Thus, the development of sensitive THz SIS mixers requires the use of novel stripline materials such as Al [2,3], NbN [4], or NbTiN [5,6,7]. To-date, the best results in this frequency range have been obtained with Nb SIS junctions in combination with Al striplines, with the best-reported sensitivity being $T_{N, \text{uncorrected}} = 840$ K at 1042 GHz [3]. Although it has been predicted that this sensitivity could be enhanced by the use of junctions with a smaller sub-gap current [8], losses in the Al striplines are expected to limit the optimum noise temperature of this device geometry to $T_N \sim 500$ -600 K [8,9]. A significant improvement upon these results likely requires the use of a low-loss superconducting stripline material with a frequency gap larger than 1.1-1.2 THz. In particular, it is hoped that the integration of NbTiN strip-lines with Nb-based SIS junctions will enable the development of low noise SIS receivers in the 0.8-1.2 THz frequency range. With this in mind, NbTiN films, which have been used for thin-film coated RF cavities for high-energy accelerators [5], have recently been introduced as a stripline material for SIS mixers [6,7,10].

In this paper we discuss the DC and RF properties of SIS mixers in which Nb junctions are integrated with either NbTiN striplines or a combination of NbTiN and Al striplines. First, an examination of their DC current-voltage characteristics allows us to evaluate the degree to which the trapping of heat in the Nb junction electrodes is a problem in these devices. Next, we present a comparison of the measured and predicted spectral response of several devices as one means of evaluating the behaviour of NbTiN as a stripline material at high frequencies. Additionally, we present what we believe to be the first reported high frequency (0.9-1 THz) heterodyne measurements of NbTiN stripline devices. Finally, we discuss the significance of these results in view of the ongoing work to develop sensitive SIS mixers for the 0.8-1.2 THz range.

2. Device Fabrication

As described in [10], Nb/Al-AlO_x/Nb junctions are integrated with NbTiN and Al striplines following a process similar to that previously developed for the fabrication of Al stripline devices [11]. Figure 1 shows the layer structure and the stripline geometry of the devices discussed in this paper. The devices are fabricated using a mask set that was originally designed for Nb and Al stripline devices in the 400-1200 GHz range. In this mask layout, the mixers are equally split between the end-loaded stripline geometry shown in Figure 1b and the $\frac{1}{4}$ - λ stripline geometry shown in Figure 1c. Table 1 summarizes the layer parameters for the three fabrication runs from which devices are taken.

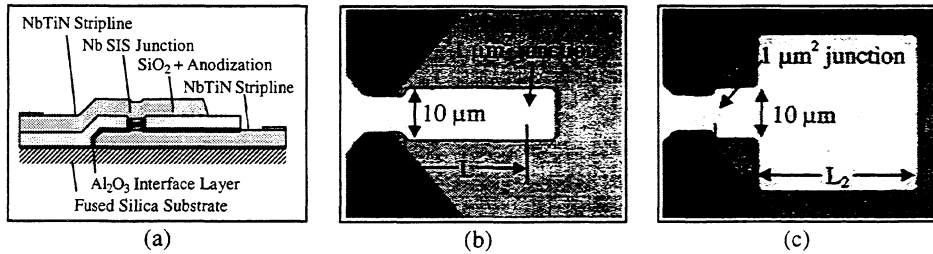


Figure 1 - a) device cross-section, b) optical microscope image of an end-loaded stripline device, where the stripline length is varied to obtain a range of resonant frequencies ($L = 15\text{-}120\ \mu\text{m}$), c) optical microscope image of a $\frac{1}{4}\text{-}\lambda$ stripline device, where L_1 and L_2 are varied to obtain a range of resonant frequencies ($L_1 = 3\text{-}50\ \mu\text{m}$ and $L_2 = 20\text{-}75\ \mu\text{m}$).

Past work has shown that there is a strong inverse correlation between compressive stress and resistivity in NbTiN films deposited at room temperature [5,6,10]. Although films can be obtained with resistivities of $\sim 80\ \mu\Omega\text{-cm}$, their high compressive stress ($> 2.5\ \text{GPa}$) precludes their integration with Nb SIS junctions. For this reason, the NbTiN films used here have a nominal resistivity of $\sim 110\ \mu\Omega\text{-cm}$, $\sim 0.5\ \text{GPa}$ of compressive stress, and a transition temperature of $14.4\ \text{K}$ [10].

Table 1 - Layer parameters for the three fabrication runs

Batch	Bottom Wiring	Trilayer (*)	Dielectric	Top Wiring
A	260 nm NbTiN	23' x 10 mTorr O ₂	250 nm SiO ₂	400 nm NbTiN
B	300 nm NbTiN	23' x 10 mTorr O ₂	250 nm SiO ₂	250 nm Al + 100 nm Nb
C	280 nm NbTiN	20' x 6 mTorr O ₂	250 nm SiO ₂	400 nm NbTiN

*oxidation parameters only, trilayer = 90 nm Nb + 6 nm Al + oxidation + 90 nm Nb

3. Measurement Configuration

DC current-voltage characteristics are obtained at $4.2\ \text{K}$ by 4-point dipstick measurements in a magnetic field for cancellation of the Josephson effect. Tuning the magnetic field allows the identification of resonant features in the sub-gap current at voltages corresponding to the resonant frequency of the junction plus microstrip tuning structure, according to the Josephson relation ($484\ \text{GHz/mV}$).

After DC testing, the substrate is polished to $40\text{-}\mu\text{m}$ thickness for testing in a 1-THz waveguide mixer block with a 120 by $240\ \mu\text{m}^2$ waveguide and a 90 by $75\ \mu\text{m}^2$ substrate channel [2]. A $15\ \mu\text{m}$ mylar beamsplitter is used to couple the local oscillator and blackbody signal power through a Teflon lens, a $100\ \mu\text{m}$ Mylar window and a $200\ \mu\text{m}$ quartz heat filter at $77\ \text{K}$. A diagonal horn is used to couple radiation into the waveguide and a contacting backshort is used as a mechanical tuning element. A Fourier transform spectrometer is used to measure the mixer bandwidth and centre frequency

with the junction operated as a direct detector. The heterodyne sensitivity of the receiver is measured using a standard 293-K / 77-K hot-cold measurement with a Carcinotron plus tripler as a local oscillator in the 840-930 GHz range and a BWO local oscillator in the 900-1100 GHz range.

4. Heating Effects in DC Current-Voltage Characteristics

Current-voltage characteristics of four " $1\text{-}\mu\text{m}^2$ " junctions are shown in Figure 2 a-d, with the average device parameters for each batch summarized in Table 2. As can be seen in Figures 2a and 2b, the lower current-density devices ($6.3\text{-}6.5\text{ kA/cm}^2$) have a relatively small amount of sub-gap leakage current, with a sharp current rise at the gap voltage. Due to the higher current-density of devices from batch C (12 kA/cm^2), a significant amount of sub-gap leakage current is seen in the current-voltage characteristic in Figure 2c. The marked features in the sub-gap currents of the devices seen in Figures 2a-c are due to resonances of the junctions' AC Josephson radiation (484 GHz/mV) with

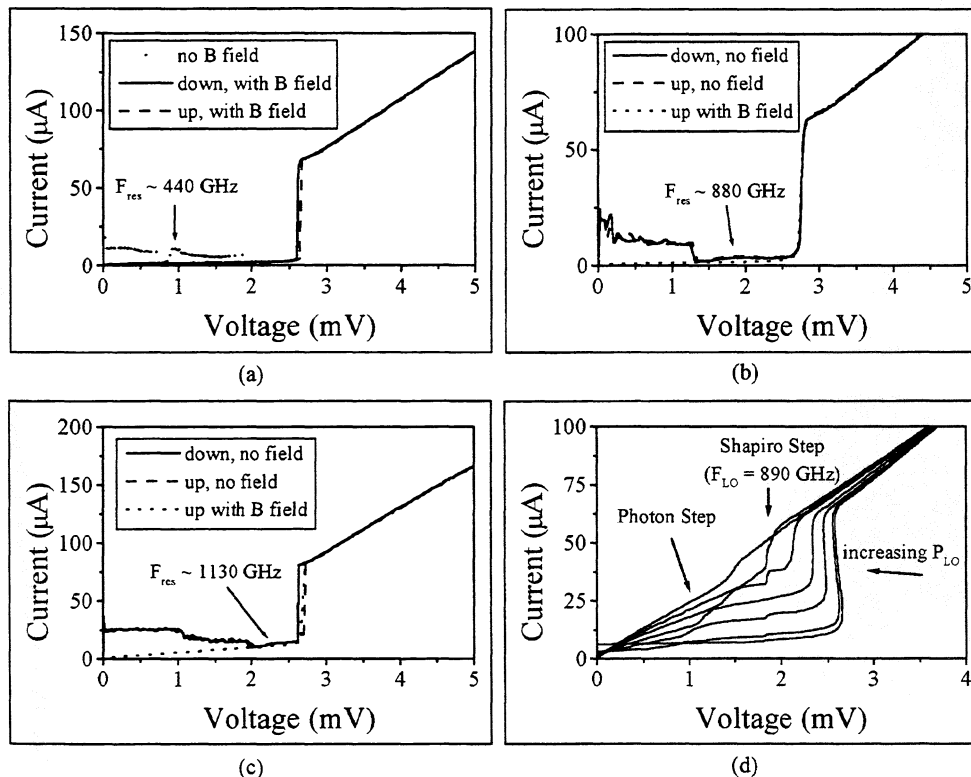


Figure 2 - sample I-V characteristics of four junctions (a-c in voltage-bias mode, d in current-bias mode): a) a 6.5 kA/cm^2 , $\frac{1}{4}\text{-}\lambda$ stripline device with two NbTiN wires, b) a 6.3 kA/cm^2 end-loaded stripline device with one NbTiN and one Al wire, c) a 12 kA/cm^2 , end-loaded stripline device with two NbTiN wires, d) a 12 kA/cm^2 , end-loaded device with NbTiN striplines mounted in the 1-THz mixer block: unpumped and with 6 increasing levels of 890 GHz local oscillator power. Note the decrease in V_{gap} and increase in $V_{photon\ step}$ with increasing LO power.

Table 2 - DC current-voltage characteristic summary

Batch	Wiring	V_{gap} (mV)	$R_n \cdot A$ ($\Omega \cdot \mu\text{m}^2$)	J_c (kA/cm ²)	A (μm^2)	$R_{2.0 \text{ mV}}/R_n$
A	NbTiN	2.65-2.72	32	6.5	0.9-1.0	~ 32
B	NbTiN - Al	2.68-2.81	35	6.3	0.6-0.9	~ 35
C	NbTiN	2.63-2.72	18	12	0.5-0.8	~ 10

the RF stripline structure. The correlation between the measured and predicted resonant frequencies will be discussed in more detail in section 5 of this paper.

From the data in Table 2, it is seen that the gap voltage and resistance ratio, $R_{2.0 \text{ mV}}/R_n$, are somewhat lower for devices with two NbTiN striplines, as compared with devices with one NbTiN and one Al stripline. Additionally, a significant amount of hysteresis can be seen at the gap voltage in devices with two NbTiN striplines (Figures 2a and 2c). These effects can be attributed to Joule heating of the junction electrodes, enhanced primarily by quasi-particle trapping at the Nb/NbTiN interfaces [12]. Further evidence of heating in junctions with two NbTiN wires is seen in Figure 2d, in which the current-voltage characteristics of a device mounted in the 1-THz mixer block are compared for a range of 890 GHz pumping powers. From this figure, it can be seen that the gap voltage decreases and the first photon step moves to higher voltages with increasing pump power.

Using the gap voltage to estimate the effective electron temperature in the Nb electrodes, it is possible to estimate the relationship between the junction temperature and the dissipated Joule power at the gap voltage for the unpumped and pumped current-voltage curves in Figure 2d. The calculated relationship between junction temperature and DC power is seen in Figure 3a. The observed back-bending in the unpumped curve is used to estimate the dependence of junction temperature on heating power by assuming that $V \sim V_{\text{gap}}(T)$ in the back-bending region. For each of the six pumped curves, a temperature is estimated from either the maximum voltage at the bottom of the gap (for the three curves in which back-bending is observed) or the point of maximum slope (for the remaining three curves). Comparing the estimated electron temperature versus DC power for the pumped and unpumped curves, it is clearly seen that the observed junction temperature can not be explained by Joule heating alone — RF power must also be dissipated in the junction. If the temperature is assumed to follow the approximately linear dependence on total power observed for the unpumped junction, it is possible to estimate the amount of dissipated RF power. In particular, for the third pumped curve in Figure 2d, it is estimated that, in addition to Joule heating, ~ 200 nW of RF power must be dissipated in the junction to raise the effective electron temperature to 6.5 K.

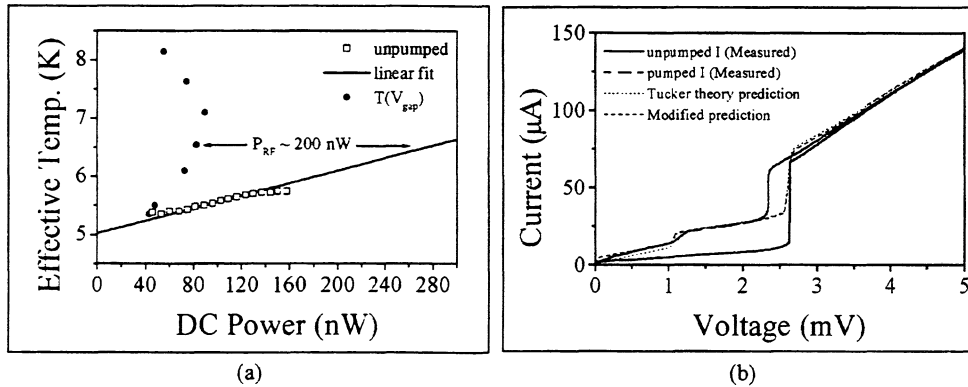


Figure 3 - (a) Effective electron temperature versus DC power calculated from the pumped current-voltage curves in Figure 2d, using V_{gap} as a measure of temperature. The set of points for the unpumped curve is generated from the back-bending at the gap voltage by assuming that $V - V_{\text{gap}}(T)$ in this region. The temperatures of the pumped junctions are estimated using either the maximum voltage at the bottom of the gap (for curves with back-bending) or the point of maximum slope. (b) Results of a Tucker theory calculation to estimate the LO power needed to generate the measured pumped curve (third pumped curve from Figure 2d chosen due to the absence of a Shapiro step).

The estimated RF dissipation in the junction can be compared with the RF power needed to generate the measured photon-assisted tunneling current, using the RF voltage-match method [13] to determine the junction's embedding impedance and the Tucker theory [14] to calculate the pumped current-voltage curves. Figure 3b presents the measured and calculated pumped current-voltage curves for the third pumping level in Figure 2d (the only curve in which the Shapiro step is negligibly small). From this calculation, it is estimated that 180 nW of RF power is needed to generate the observed photon-assisted tunneling current. However, due to heating of the junction by the absorption of RF power, the observed current increase due to pumping is actually a sum of photon-assisted tunneling and an increase in the thermally generated quasi-particle current. This may explain why the calculated pumped curve under-estimates the current in the region below the photon step, as seen in Figure 3b. The correlation between the calculated and measured curves below the photon step is improved if 5 μA is added to the unpumped sub-gap current (6.5% of the current at the gap). In this case, the pumping power needed to match the measured and calculated curves is estimated as 150 nW. Thus, it can be said that the RF power contributing to the observed photon-assisted tunneling is $\sim 150\text{-}180$ nW, which is comparable to the estimated RF dissipation in the junction, 200 nW.

5. Measured and Predicted Spectral Response

Figures 4a-c present the measured FTS spectra for three NbTiN stripline devices operated in a direct detection mode. Also seen in these figures are the calculated spectral response and a description of the stripline geometry for each device. From Figures 4a and 4b it can be seen that the high-frequency end-loaded devices have broad tuned

bandwidths, with central frequencies of ~ 900 and 1000 GHz, fixed-tuned bandwidths as high as 100-120 GHz (Figure 4a), and significant responses up to 1150-1200 GHz (Figure 4b). To the best of our knowledge, this is the highest frequency at which a direct detection response has been reported in NbTiN stripline devices. As seen in Figure 4c,

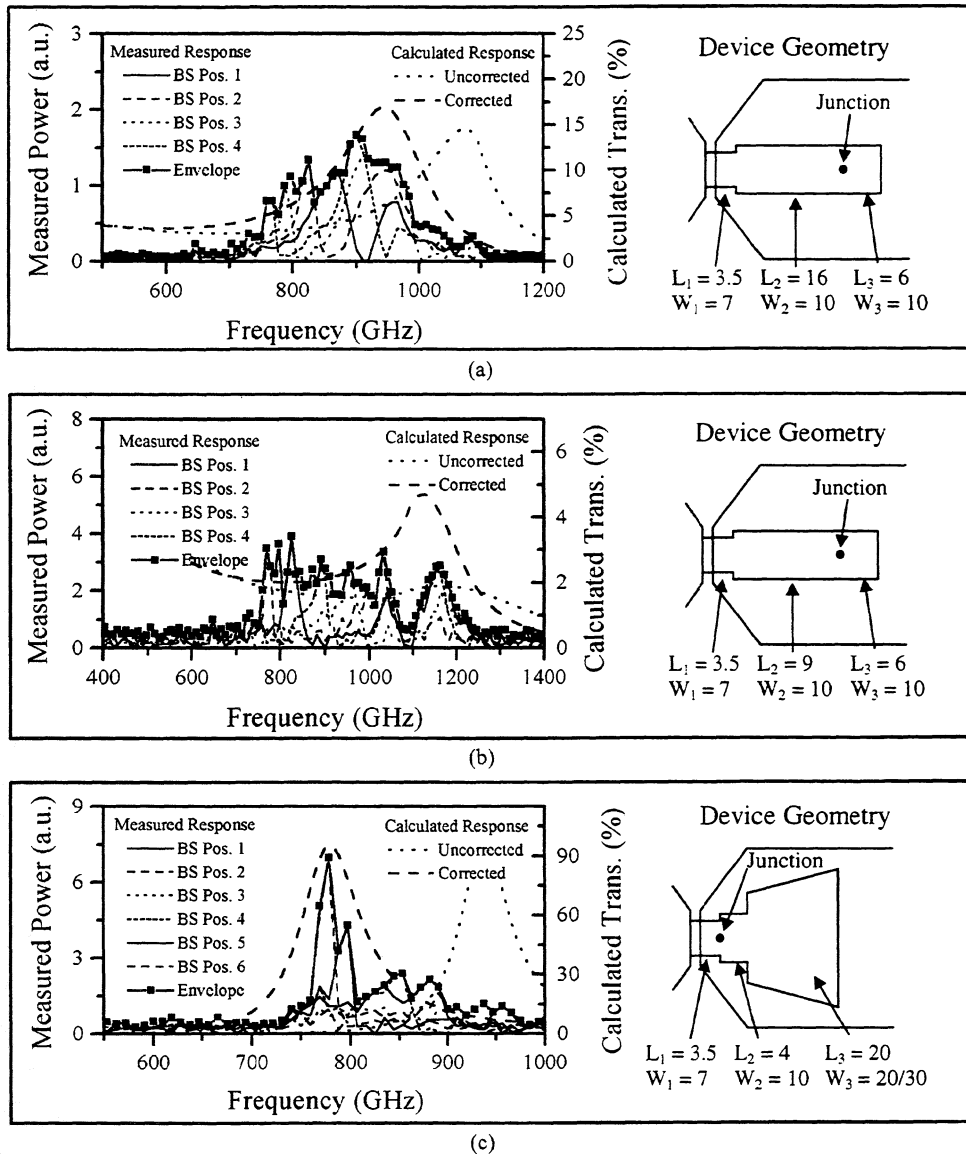


Figure 3 - Spectral response of three Nb SIS junctions integrated with NbTiN striplines. Seen here for each device are measured FTS spectra for a range of backshort positions, calculated resonance spectra for a match to a 50 Ω source impedance, and a sketch of the corresponding device geometry (all dimensions in μm). (a) response of an end-loaded stripline with a $0.6 \mu\text{m}^2$, 6.5 kA/cm^2 junction, (b) response of an end-loaded stripline with a $0.6 \mu\text{m}^2$, 6.5 kA/cm^2 junction, and (c) response of a $1/4\text{-}\lambda$ stripline device with a $0.6 \mu\text{m}^2$, 12 kA/cm^2 junction.

the $\frac{1}{4}\lambda$ stripline device has a much sharper spectral response than the measured end-loaded devices, with a peak frequency of 775 GHz and a fixed-tuned bandwidth of < 50 GHz. The cause of the dip observed at ~ 1100 GHz in Figure 4b is not known (the measurement is performed in a vacuum FTS to minimize absorption by water vapour). However, it may be a waveguide effect, possibly related to the fact that the substrate thickness is $\sim \frac{1}{4}\lambda$ at 1100 GHz.

Included in each of Figures 4a-c are two calculations of the predicted transmission of power to the junction from a 50Ω source located at the input of the stripline. In all cases, the surface impedance of the NbTiN wiring layers is calculated using the local limit approximation for the surface impedance as a function of the frequency-dependent conductivity, σ_s . This conductivity is determined from the Mattis-Bardeen formulation for $\sigma_s = \sigma_1 - j \cdot \sigma_2$ in the extreme anomalous limit [1], using the previously measured parameters for our films ($\rho_{n,DC} \sim 110 \mu\Omega\text{-cm}$, $T_c = 14.4$ K [10]). The uncorrected transmission curve is calculated from the actual device geometry, and can be seen to predict, in each case, a resonance frequency significantly higher than the measured central frequency. The correlation between the measured and predicted spectra is significantly improved if an extra length of $3.7 \mu\text{m}$ is added to the stripline on each side of the junction, as seen from the "corrected" calculations in Figures 4a-c. This effect is seen to be particularly significant for the $\frac{1}{4}\lambda$ stripline device in Figure 4c, due to the low length-to-width ratio of the striplines in this structure. An examination of the sub-gap current resonances for a number of end-loaded and $\frac{1}{4}\lambda$ devices finds a similar correlation between the measured voltages and the resonant frequency predicted by the corrected calculation (for resonances from 350 GHz to 1100 GHz).

6. Heterodyne Response

Figure 5 shows the results of a hot/cold measurement of a NbTiN stripline device pumped at 930 GHz at a mixer block temperature of 4.5 K. To the best of our knowledge, this is the highest frequency at which heterodyne sensitivity in an SIS mixer with NbTiN striplines has been reported to-date. Figure 5a presents the pumped and unpumped current-voltage characteristics, together with the hot and cold IF output powers as a function of bias voltage. Figure 5b presents the corresponding Y-factor and uncorrected noise temperatures as a function of bias voltage. The measured device is a $0.6 \mu\text{m}^2$, 12 kA/cm^2 junction with the same end-loaded stripline geometry as that seen in Figure 4a.

From Figure 5b, it is seen that the minimum receiver noise temperature calculated from the measured IF output powers is ~ 1000 K DSB. Correcting for loss in the $15\text{-}\mu\text{m}$ Mylar beamsplitter yields a corrected receiver noise temperature of ~ 900 K. However, because this sensitivity is calculated at 2.1-2.2 mV, in the region of the small side-peak in the IF output power, it is sensitive to averaging and small offsets between the hot and cold curves. A manually chopped hot-cold measurement at an optimum bias point

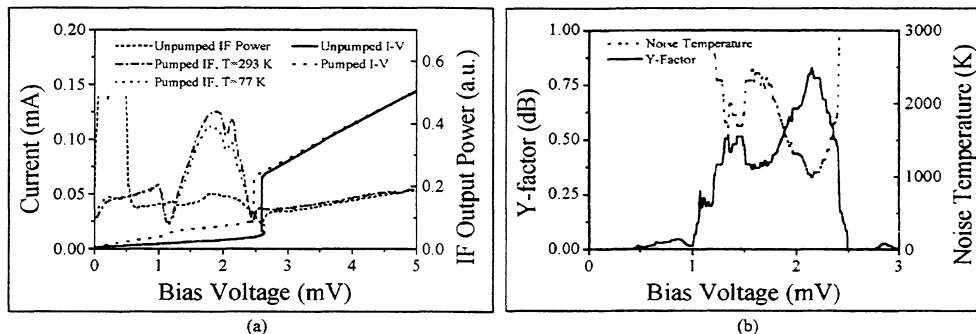


Figure 5 - Noise temperature measurements of a 12 kA/cm^2 , end-loaded stripline device at 930 GHz and a mixer block temperature of 4.5 K. (a) unpumped and pumped current-voltage curves and IF output powers for a hot (293 K) and a cold (77 K) blackbody load. Note that the dip at 2-2.1 mV is too high in voltage to be due to a Shapiro step. (b) calculated Y-factor and noise temperature within the sub-gap region.

produces a Y-factor of 0.51 dB, which corresponds to a corrected noise temperature of 1540 K. Pumping on the helium bath is seen to improve the corrected noise temperature to 830 K at a mixer block temperature of 3.3 K, also for a manually chopped hot/cold measurement at a fixed bias point.

These receiver measurements are complicated by the already mentioned suppression of the gap voltage by Joule heating and the absorption of RF power. This effectively reduces the bias range available for high frequency measurements. Furthermore, an observed instability in the magnetic field needed to suppress the Josephson effect adds an additional degree of complication — at these frequencies the Shapiro step (at 2.07 mV/THz) lies in the centre of the already reduced bias range. As a result of these effects, it is not possible to produce reliable heterodyne measurement results at 1040 GHz for the device whose spectral response is seen in Figure 4b.

7. Discussion and Conclusions

It has been seen that the gap voltage of Nb junctions integrated with NbTiN striplines is suppressed by the trapping of Joule heat and absorbed local oscillator power. For a junction with a current density of 12 kA/cm^2 , the unpumped gap voltage is 2.7 mV, while the application of 890 GHz local oscillator power further reduces the gap voltage to 2.3-2.4 mV for pumping levels typically used in a heterodyne experiment. This corresponds to effective electron temperatures of 5.2 K for the unpumped junction and ~ 6.5 K for the pumped junction. This large temperature difference can only be explained if ~ 200 nW of local oscillator power is dissipated in the pumped junction. Furthermore, from Tucker theory, it is estimated that 150-180 nW of local oscillator power are needed to generate the observed photon-assisted tunnelling. Although these estimates are not accurate enough to draw firm conclusions, the excess dissipated power could represent RF loss in the Nb electrodes due to the incident radiation being higher in frequency than

the Nb gap frequency. In a heterodyne measurement, such a loss would result in a reduction in device sensitivity for frequencies above ~ 700 GHz.

Heating of the Nb junctions by a combination of DC and RF power will affect mixer performance in at least three ways:

1. an increase in mixer noise due to an increase in the thermally generated sub-gap leakage current
2. a reduction in the maximum frequency which can be efficiently detected by the junction ($F_{\max} \sim V_{\text{gap}} \cdot 484 \text{ GHz/mV}$)
3. a reduction in the bias range available during receiver measurements due to the reduced gap voltage and increase in the voltage of the the first photon step from the negative branch of the I-V curve

The observed trapping of heat in the junction electrodes can be attributed primarily to quasi-particle trapping at the Nb/NbTiN interface. Because of this effect, heat may not escape the Nb electrodes through electron diffusion. Rather, heat must be transferred to the phonons in the Nb electrodes through the electron-phonon interaction. Heat may then be transferred to the NbTiN, and eventually the substrate, through phonon-phonon interactions. Further study is needed to identify the rate-limiting step(s) in this process, in order that the device geometry can be modified to reduce the observed heating effects. For example:

1. Replacing one NbTiN wire with Al will eliminate one trapping interface, at the cost of increased stripline losses.
2. The use of the recently introduced Nb/Al-AlN_x/NbTiN junction structure [15] will also eliminate one trapping interface.
3. If the barrier to heat transfer from NbTiN to the substrate (the Kapitza resistance) is high, an Al layer between the NbTiN and the substrate may enhance the cooling of phonons in the NbTiN.
4. The effect of THz radiation being absorbed in the Nb electrodes may be reduced by a change in the junction geometry to shorten the current path within the Nb.

As mentioned previously, the reduction of the available bias range is further complicated by the apparent instability of these devices with respect to the magnetic field needed to suppress the Josephson effect. This instability means that it is desirable to bias the device well away from the Shapiro step (at 2.08 mV/THz). However, this is difficult because in the frequency range of interest, around 1 THz, this voltage lies within the already reduced bias range. Although the cause of the observed instability has not been examined, it is thought that flux trapping within the NbTiN wires may be responsible.

The frequency response of Nb SIS junctions integrated with NbTiN striplines has been compared with model calculations to evaluate the high frequency behaviour of NbTiN. These measurements include the first reported measurements of direct detection response above 1.1 THz in devices with NbTiN striplines. The qualitative agreement between the measured and calculated central frequency for the end-loaded devices is generally good. This qualitative agreement is seen to break down for the higher frequency $\frac{1}{4}\lambda$ stripline devices, likely due to the small length-to-width ratios in the striplines in these devices. However, relatively good quantitative agreement for all devices can be obtained by the addition of an extra stripline length of $3.7\ \mu\text{m}$ on each side of the junction. This extra length may approximate the effect of the discontinuity in width between the $1\text{-}\mu\text{m}$ junction and the $10\text{-}\mu\text{m}$ stripline. Thus, absolute confirmation of the high frequency properties of NbTiN striplines will require either the calculation of the two-dimensional current distribution in the stripline geometries used here, or the testing of new devices with geometries which are much less sensitive to the effects of discontinuities. In general, though, the results presented here, together with those of previous studies [6,7] indicate that the frequency response of NbTiN striplines can be reasonably well predicted by the Mattis-Bardeen theory for a superconductor in the extreme anomalous limit.

The receiver sensitivity measurement reported here is, to the best of our knowledge, the first heterodyne measurement above 900 GHz of a Nb SIS junction integrated with NbTiN striplines. It has been shown that an end-loaded device with a high current-density junction yields a sensitivity of $T_{N, \text{corrected}} \sim 830\ \text{K DSB}$ at 930 GHz, at a mixer block temperature of 3.3 K. Although this sensitivity remains 4-5 times higher than required for HIFI, it approaches the best sensitivity reported for Al stripline devices in this frequency range — $T_{N, \text{uncorrected}} = 840\ \text{K}$ at 1040 GHz and a bath temperature of 2.5 K [3].

Unfortunately, the DC and RF heating of the junction complicate the use of the standard Tucker theory to determine the contributions of individual elements to the measured receiver noise. Thus, it is difficult to draw further conclusions from these heterodyne results at this time. However, three general comments can be made. First, it is noted that, due to the effects of Andreev reflection enhanced shot noise [9,16], it should be possible to improve upon these results by the use of a junction with a lower current-density than that used here ($12\ \text{kA/cm}^2$). Furthermore, the dewar window and the 77 K heat filter are found to have significant losses at 930 GHz ($\sim 19\%$ and 35% , respectively), and thus, are likely responsible for a significant contribution to the receiver noise. Finally, FTS measurements show this device to have relatively broad fixed-tuned bandwidths (up to 140 GHz, similar to Figure 4a), which may be the result of poor matching of the incoming radiation to the junction impedance. Indeed, calculations of the coupling of radiation from a $50\ \Omega$ source to the junction predict only $\sim 25\%$ coupling for this geometry, although the use of a tunable backshort makes it difficult to know what the junction's real embedding impedance is. In general, these calculations indicate that other stripline geometries, such as the $\frac{1}{4}\lambda$ stripline, may give much better coupling at these

high frequencies. Thus, although these initial results are promising, further measurements of a range of devices with different resonant frequencies and stripline geometries are needed before the benefits of using NbTiN as a stripline material can be fully quantified.

8. Acknowledgements

The authors would like to thank S. Bakker, B. Wolfs, D. Nguyen, and H. Schaeffer for their technical assistance and A. Baryshev, P. Dieleman, W. Ganzevles, N. Whyborn, and D. Wilms Floet for numerous discussions. The authors would also like to thank H. LeDuc, J. Stern, and B. Bumble of the Jet Propulsion Laboratory's Center for Space Microelectronics Technology and J. Zmuidzinas of the California Institute of Technology, for exchanging information regarding the integration of NbTiN in Nb-based SIS mixers. This work is supported in part by the Stichting voor Technische Wetenschappen (STW), the Nederlandse Organisatie voor Wetenschappelijk Onderzoek (NWO), and the research program of the European TMR network for Terahertz electronics (INTERACT).

9. References

- [1] D.C. Mattis and J. Bardeen, "Theory of the anomalous skin effect in normal and superconducting metals", *Phys. Rev.*, vol. 111, p. 412, July 1958.
- [2] H. van de Stadt, A. Baryshev, P. Dieleman, Th. de Graauw, T. M. Klapwijk, S. Kovtonyuk, G. de Lange, I. Lapitskaya, J. Mees, R.A. Panhuyzen, G. Prokopenko, and H. Schaeffer, "A 1 THz Nb SIS heterodyne mixer with normal metal tuning structure", *Proc. 6th Internat. Symp. On Space Terahertz Technology*, CIT, PC, p. 66, March 1995.
- [3] M. Bin, M.C. Gaidis, J. Zmuidzinas, T.G. Phillips, and H.G. LeDuc, "Low-noise 1 THz niobium superconducting tunnel junction mixer with a normal metal tuning circuit", *Appl. Phys. Lett.*, vol. 68 (12), p. 1714, March 1996.
- [4] Y. Uzawa, Z. Wang, A. Kawakami "Terahertz NbN/AlN/NbN mixers with Al/SiO/NbN microstrip tuning circuits", *Proc. 9th Internat. Symp. on Space Terahertz Technology*, CIT, PC, p. 273, March 1998.
- [5] R. Di Leo, A. Nigro, G. Nobile, R. Vaglio, "Niobium-titanium nitride thin films for superconducting rf accelerator cavities". *J. Low Temp. Phys.*, vol. 78, p. 41, November 1990.
- [6] J.A. Stern, B. Bumble, H.G. LeDuc, W. J. Kooi, J. Zmuidzinas, "Fabrication and dc-characterization of NbTiN based SIS mixers for use between 600 and 1200 GHz", *Proc. 9th Internat. Symp. on Space Terahertz Technology*, CIT, PC, p. 305, March 1997.

- [7] J.W. Kooi, J.A. Stern, G. Chattopadhyay, H.G. LeDuc, B. Bumble, and J. Zmuidzinas, "Low-loss NbTiN films for THz SIS mixer tuning circuits", *Int. J. of IR and MM Waves*, vol. 19, 1998.
- [8] P. Dieleman, T.M. Klapwijk, J.R. Gao, and H. van de Stadt, "Analysis of Nb superconducting-insulator-superconducting tunnel junctions with Al striplines for THz radiation detection", *IEEE Transactions on Applied Superconductivity*, vol. 7, p. 2566, 1997.
- [9] P. Dieleman, J.R. Gao, and T.M. Klapwijk, "Doubled shot noise in niobium SIS mixers", *Proc. 9th Internat. Symp. on Space Terahertz Technology, CIT, PC*, p. 235, March 1998.
- [10] N.N. Iosad, B.D. Jackson, T.M. Klapwijk, S.N. Polyakov, P.N. Dmitriev, and J.R. Gao, "Optimization of rf- and dc-sputtered NbTiN films for integration with Nb-based SIS Junctions", to be published in *IEEE Transactions on Applied Superconductivity*, June 1999.
- [11] J.R. Gao, S. Kovtonyuk, J.B.M. Jegers, P. Dieleman, T.M. Klapwijk, and H. van de Stadt, "Fabrication of Nb-SIS mixers with UHV evaporated Al striplines", *Proc. 7th Internat. Symp. on Space Terahertz Technology, CIT, PC*, p. 538, March 1996.
- [12] N.E. Booth, "Quasiparticle trapping and the quasiparticle multiplier", *Appl. Phys. Lett.*, vol. 50, p. 293, Feb. 1987.
- [13] A. Skalare, *International Journal of Infrared and Millimeter Waves*, vol. 10, p. 1339, 1989.
- [14] J.R. Tucker and M.J. Feldman, "Quantum detection at millimeter wavelengths", *Reviews of Modern Physics*, Vol. 57, No. 4, p. 1055, Oct. 1985.
- [15] B. Bumble, H.G. LeDuc, and J.A. Stern, "Fabrication of Nb/Al-Nx/NbTiN junctions for SIS mixer applications above 1 THz", *Proc. 9th Internat. Symp. on Space Terahertz Technology, CIT, PC*, p. 295, March 1998.
- [16] P. Dieleman, H.G. Bukkems, T.M. Klapwijk, M. Schicke, and K.H. Gundlach, "Observation of Andreev reflection enhanced shot noise", *Appl. Phys. Lett.*, vol. 79, p. 3486, 1997.